EUROPHYSICS LETTERS 1 June 2004

Europhys. Lett., **66** (5), pp. 667–673 (2004)
DOI: 10.1209/epl/i2003-10242-8

Invagination during the collapse of an inhomogeneous spheroidal shell

L. PAUCHARD[1](*) and Y. COUDER[2]

[1] *Laboratoire Fluides, Automatique, Systèmes Thermiques (associé au CNRS et aux Universités Paris 6 et Paris 11) Bâtiment 502, Campus Universitaire d'Orsay, 91405 Orsay Cedex, France*
[2] *Laboratoire de Physique Statistique (associé au CNRS et aux Universités Paris 6 et Paris 7) Ecole Normale Supérieure - 24 rue Lhomond, 75231 Paris Cedex 05, France*

(received 7 August 2003; accepted in final form 12 March 2004)

PACS. 46.32.+x – Static buckling and instability.
PACS. 82.70.Dd – Colloids.
PACS. 62.10.+s – Mechanical properties of liquids.

Abstract. – The collapse of shell-shaped membranes due to buckling is investigated experimentally using droplets of latex suspension left to dry. The evaporation of water, limited by diffusion in air, first leads to the formation, on the surface, of a spheroidal envelope of gel. During the later evolution, spontaneous buckling of this envelope occurs. The later evolution leads to a large-amplitude invagination and for certain concentrations to a transition to a toroidal shape. This specific evolution of a spheroidal envelope, linked with its inhomogeneous mechanical properties, is similar to that observed during the gastrulation of sea-urchin embryos.

In the present article we address the problem of the collapse of spherical shells under external pressure. It is relevant to engineering situations (collapse of concrete domes, vessels, etc.) [1–3] as well as to biomechanics [4]. In the latter case, it is of particular interest in the context of gastrulation, the process during which an initially spherical embryo undergoes an invagination (the precursor of the formation of the inner organs). Experimentally, the collapse of spherical shells is often investigated during the crushing of hollow spheres of, *e.g.*, copper [1,2] or nanocapsules of polymeric solutions [5]. It is characterised by the formation of several depressions where the curvature is reversed so that the sphere becomes wrinkled. This phenomenon, also observed during the drying of green peas or apples, appears very different from the unique large-amplitude invagination which characterises gastrulation. Another type of experiment concerns the drying of a sessile drop formed of a colloid (or a polymer solution) [6,7] deposited onto a substrate. The drying first leads to the formation of a superficial rigid skin. Later, this shell buckles leading to inversions of curvature. However, in the situations hitherto investigated [6,7], the skin was glassy so that its increasing rigidity rapidly impeded a continuation of the buckling process.

(*) E-mail: pauchard@fast.u-psud.fr

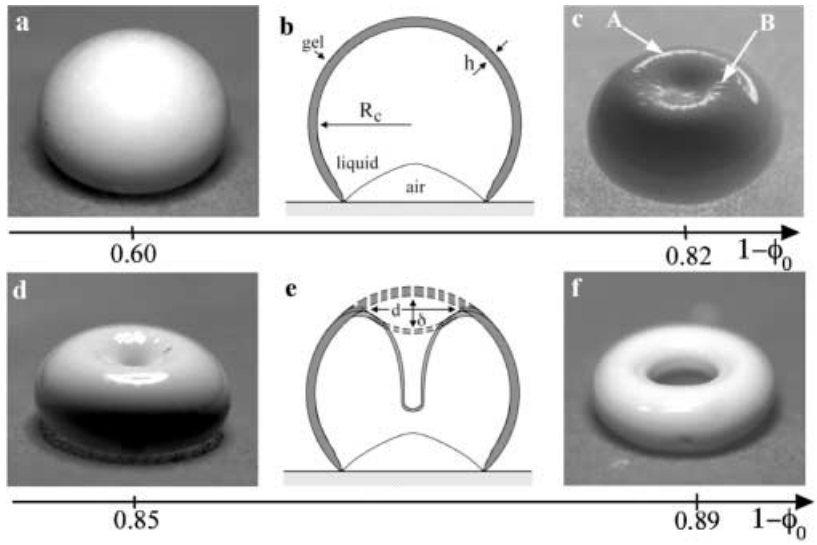

Fig. 1 – Digitised images of latex suspension droplets deposited on super hydrophobic surfaces at the final stage of desiccation. The drops meridian radii are 1.2 mm. The photographs show the various shapes obtained for different values of the initial particle volume fraction ϕ_0. (a) At large particles concentration, the shrinkage is uniform. (c) and (d) Photographs of the collapse due to a local buckling. The formation of a circular ridge is shown by arrow A in (c). All around this depression, a fine structure of radial wrinkles (arrow B) forms, having a length scale induced by bending stiffness in agreement with ref. [8]. (f) The toroidal shape obtained for the most diluted solutions. The sketches (b) and (e) correspond to (a) and (d), respectively, and show the non-uniform thickness of the membrane resulting from the local evaporation rate as well as the formation of an air bubble from below.

Here we studied the collapse of the spheroidal shell formed by evaporation at the surface of a drying droplet of a colloidal suspension. There are two specificities to the present work. i) We use a super-hydrophobic substrate [9], so that relatively large drops remain spheroidal when deposited onto it. ii) With the chosen material, the skin remains porous thus allowing further evaporation. The drying itself is well defined, being controlled by the diffusion of water vapour in air [10]. This is a model system with well-controlled physico-chemical properties and in which the theory of membranes elasticity can be applied [11]. The degree of deformation of such droplets during drying varies. It is naturally a function of the volume fraction of the particles and is driven by the pressure gradient inside and outside the spheroidal shell. Varying the water concentration of the suspensions, different shapes are observed at the final stage of the desiccation process. For high concentrations of particles, the droplet just shrinks and little change in shape is observed during the evaporation (fig. 1a). For weaker concentrations an inversion of the curvature takes place at the top of the spherical droplet (fig. 1c). When shrinkage is stronger, this inverted region grows into a single invagination (fig. 1d). Finally, at very low concentration there is a change in topology and transition to a toroidal shape (fig. 1f).

The experiments were carried out with aqueous suspensions of rigid latex particles ($a =$ 100 nm in diameter) having a high-particle volume fraction (for the most concentrated, initially, $\phi_0 = 0.40$). Since neither sedimentation nor particles aggregation takes place, the suspensions are stable without water loss. The nearly spheroidal geometry is obtained by depositing droplets on super hydrophobic substrates; these surfaces are sprayed with Lycopodium spores which form a rough texture in which air remains trapped when a drop is

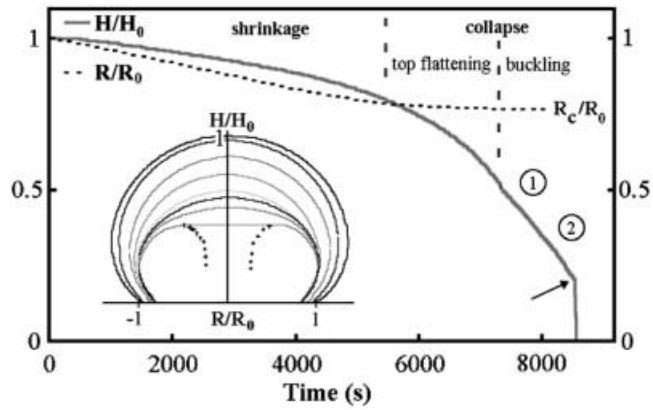

Fig. 2 – Time variations of the dimensionless meridian radius, R/R_0 (dashed line), and dimensionless apex height, H/H_0 (grey line), measured for a droplet of a diluted suspension ($1-\phi_0 = 0.89$). The top of the membrane shell flattens after the meridian radius reaches a constant value. Then a shape change of the shell occurs: buckling instability (region 1) before the tip of the invagination deepens (region 2). The black arrow indicates the tearing of the film separating the bubble and the tip of the invagination. Inset: superposition of dimensionless profiles measured at different times by lateral imaging except in the final stage where measurements were done using a laser sensor (the duration between two consecutive profiles is 300 s).

deposited. As a result, the contact angle of the drop on the substrate is of the order of 155° and the drop has the shape of a spheroid of revolution around the vertical axis. It is left to desiccate under controlled relative humidity and temperature (water loss is limited by diffusion of water vapour in the air).

Figure 2 shows a typical shape evolution during the evaporation of solvent. We measure the time evolution of the meridian radius R and the height H of the drop along its vertical axis. Since the evaporation rate is slow, the internal pressure remains uniform and the drop firstly shrinks nearly isotropically, as described in the inset in fig. 2. Both apex height and meridian radius linearly decrease (note that the radius of the contact base of the drop on the substrate shrinks nearly by 10% before reaching a constant value). During water loss, evaporation brings the particles onto the liquid-vapour interface where their concentration grows (see inset in fig. 3). In contrast, in the core of the drop, the particles volume fraction remains approximately equal to its initial value ϕ_0. This accumulation thus leads to the formation, near the surface, of a boundary layer through which the concentration changes. This layer has a thickness L_d limited by diffusion in the fluid. The mean gradient can thus be estimated to be $(\phi_\mathrm{S}-\phi_0)/L_\mathrm{d}$. As time passes two effects occur. The concentration ϕ_S increases and the boundary layer becomes thicker with $L_\mathrm{d} = (Dt)^{0.5}$ (where D is the diffusion coefficient of particles in the solvent). When ϕ_S reaches the gel concentration value ϕ_G, characteristic of the close packing of particles, a gelled skin forms at the surface. This skin will, from then on, behave as a thin shell. As expected, the more concentrated the suspension, the faster the gelled skin will form (this results in different rates of mass reduction due to the drying of droplets of different concentrations when compared to pure water drops). When the thin shell is formed at its surface, the drop stops shrinking transversally; as a consequence, the meridian radius, R, reaches a constant value denoted R_C, as shown in the plot for a given droplet in fig. 2. This critical value, R_C, was measured for droplets of different concentrations. As shown in fig. 3, the more diluted the solution (larger $1-\phi_0$), the lower the ratio R_C/R_0. These results can be

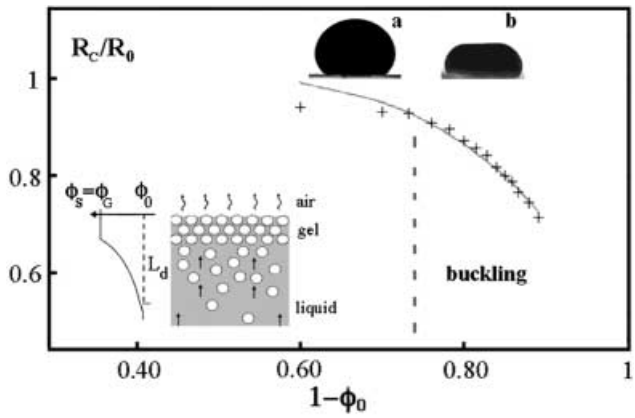

Fig. 3 – Dimensionless critical radius, R_C/R_0, characterizing the end of the droplets shrinkage *vs.* water concentration of the suspension, $1-\phi_0$. Measurements are well fitted by theory (grey line). For weak dilutions ($1-\phi_0 < 0.75$), the droplet just shrinks leading to the final side view (a) (image corresponding to a drop of initial water concentration $1-\phi_0 = 0.60$). For weaker concentrations, an inversion of the curvature takes place leading to a final side view similar to (b) (initial water concentration $1-\phi_0 = 0.80$). Inset: schematic illustration of the accumulation of particles at the air-vapour interface during the desiccation process.

explained simply by setting the solvent flux conservation at the air-vapour interface. In this way the evaporation rate is $V_E \sim S^{-1}\mathrm{d}V/\mathrm{d}t$, where S and V are, respectively, the surface and volume of the droplet at time t; V_E is deduced from measurements on the successive profiles shown in fig. 2. Also, the diffusion coefficient, D, is evaluated using the Einstein law [12].

Once the gel has formed, as the voids inside the porous skin contain free water, the main mechanism of moisture transfer is governed by the pressure gradient resulting from the capillary pressure. The later behaviour of the shell-shaped membrane is strongly influenced by the initial latex particle volume fraction.

i) For weak dilutions such as $1-\phi_0 < 0.75$, the concentration gradient near the interface is low leading to a thick, rigid, gelled skin. During later drying, the water continues flowing through the porous membrane which does not deform. This is the reason why R_C becomes independent of $1-\phi_0$ (see fig. 3). A point is reached where the shape of the drop becomes apparently constant while its weight continues to decrease. The drop being opaque, the process of this weight loss is only revealed at the end of the experiment. Examining the final solid, it is found that an air bubble has formed inside it from below [13]. It can be understood as follows. When a solid shell has formed, the stresses resulting from the drying generate a low pressure inside the whole drop. At this point, in the region of contact with the substrate, either the shell has not formed or it is very thin. In both cases, the fluid in this region is sucked in. The underlying super hydrophobic surface has a rough structure in which air usually remains trapped. Submitted to a low pressure it allows for an inward radial air flow. This air entry compensates the water loss. A bubble thus slowly grows inside the drop as shown in the schematic illustration of fig. 1b.

ii) For diluted solutions of latex particles, with $1-\phi_0 > 0.78$, the concentration gradient is larger, leading to the formation of a thinner, more elastic, membrane capable of deformation due to the decrease of its inner volume. As evaporation continues, the drop progressively flattens as described by the profiles superposition in the inset in fig. 2. This deformation is driven both by gravity, breaking the vertical symmetry, and, mainly, by the pressure gradient govern-

ing the transport of a solvent of viscosity η_0 through a porous medium of thickness h (thickness of the spheroidal envelope) and permeability k (proportional to a^2) according to Darcy law:

$$\Delta P = P_{\mathrm{i}} - P_{\mathrm{c}} = k^{-1}\eta_0 V_{\mathrm{E}} h\,; \tag{1}$$

here P_{c} denotes the capillary pressure drop, close to $2\gamma/a = 2\cdot 10^6\,\mathrm{N\,m^2}$, where γ is the air-water surface tension, and P_{i} the pressure inside the spheroidal envelope ($V_{\mathrm{E}} < 0$, typically $|V_{\mathrm{E}}| = 10^{-4}\,\mathrm{mm\,s^{-1}}$).

In the case of a thin elastic shell, of Young modulus Y, submitted to an external pressure ΔP, the two primary modes of deformation are stretching (in-plane displacement) and bending (out-of-plane displacement) [11]. By setting δ the amplitude of the deformation, also the depth of the invagination, the major contribution to the elastic energy comes from the length change in the envelope. Thus, the in-plane elastic energy scales as

$$E_{\mathrm{s}} = Yh\left(\frac{\delta}{R_{\mathrm{C}}}\right)^2 A \tag{2}$$

for the deformed surface of area A. This energy must be balanced by the work, $\Delta P(A\cdot\delta)$, exerted by the pressure ΔP. Taking into account (1) and (2), the amplitude of the deformation is expressed as $\delta_1 = k^{-1}\eta_0 R_{\mathrm{C}}^2 V_{\mathrm{E}}^2 Y^{-1}$; thus, for a given value V_{E}, the more rigid the membrane (large Y), the lower the amplitude of the deformation. This characterizes the flattening of the top of the spheroidal shell. Comparison of the theoretical amplitude of the deformation, δ_1, with measurements done at the final stage of the top flattening allows for an evaluation of the Young modulus of the gelled envelope of the order of $10^6\,\mathrm{N\,m^2}$ (in agreement with measurements performed on drying silica layers in ref. [14]). In the top flattening process, a great part of the elastic energy comes from stretching. As time passes, in the presence of such a depression, extensional deformations are not energetically favorable and bending deformation will be preferred. Thus, most of the elastic energy concentrates in a circular ridge (arrow A in fig. 1c) [15]. Hence the elastic energy is now expressed as

$$E_{\mathrm{b}} = Y'\frac{h^{5/2}\delta^{3/2}}{R_{\mathrm{C}}}\,. \tag{3}$$

Comparing E_{b} and the work of the pressure, ΔP, acting on the membrane, the amplitude of the deformation scales as $\delta_2 = k^{-2}h^{-3}\eta_0^2\, R_{\mathrm{C}}^2 A^2 Y'^{-2} V_{\mathrm{E}}^2$. The buckling process occurs in region 1 of the spatio-temporal diagram in fig. 2.

This is a classical result: it corresponds to the first instability observed in the collapse of thin spherical shells [1,2]. In this latter case, however, there is formation of several depressions in different regions of the sphere. Here, in contrast, as the system keeps shrinking, no other depression will appear. Instead, the single depression at the top of the drop deepens and forms an invaginating tube (figs. 1d and e). The origin of this behavior lies in the inhomogeneity of the shell. Indeed, the evaporation rate through the area of the convex surface decreases with decreasing curvature: this already occurs in the first stage of the top flattening process. Consequently, the flattened top part of the shell displays a lower stiffness than the rest of the envelope of gel. This can be shown by comparing the behaviors under water loss of two droplets having the same weak dilution ($1-\phi_0 < 0.75$) but placed in different environments. One of them is left to desiccate in the open while the other is located below a horizontal solid plate forming a ceiling above it. In this situation the air located between the drop and this ceiling becomes quickly saturated in water vapor and the evaporation of the top of the drop is weakened (fig. 4).

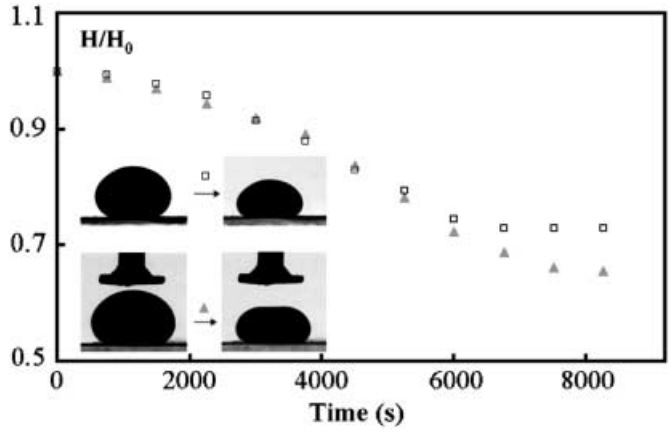

Fig. 4 – Time variations of the dimensionless apex height for two droplets having the same initial concentration ($1-\phi_0 = 0.70$) but left to desiccate below a horizontal solid plate (▲) and in the open, respectively (□). (The distance between the top of the drop and the ceiling is 200 μm at $t = 0$.)

While the drop in the open just shrinks, the drop located below a solid surface exhibits a buckling transition. In other terms, the lower stiffness induced at the top of the spheroidal shell by the weaker evaporation leads to a deformation usually observed for weak concentrations.

Moreover, above the buckled membrane, due to the concavity of the surface, the evaporation is much weaker. As a result, the solid shell remains thin in this region. It is not costly energetically for the system to force a plastic deformation of the shell in the singular region formed by the tip of the invagination. As this tip penetrates, it will meet the small bubble formed from below inside the drop (fig. 1e). In the case shown in fig. 1f, where the separating film is torn by the stresses, this leads to the formation of a torus.

The evolution of the shell membrane we observe is strikingly similar to the transition observed in embryos during the gastrulation stage. Figure 5 shows two photographs (courtesy of J. B. Morrill) of the invagination in the sea-urchin embryo (a widely studied archetype of this process) [4]. Before gastrulation, the sea-urchin blastula is a nearly spherical shell formed

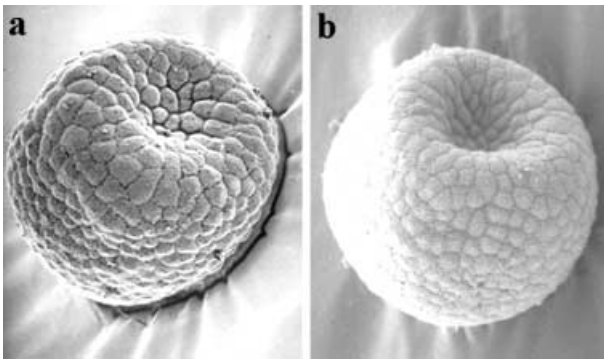

Fig. 5 – Scanning electron micrograph of external surface of the early gastrula showing the reverse of curvature of the vegetal plate (a) and the invagination into the blastocoel (b) in *Lytechinus variegatus* (500 μm in diameter). Courtesy of J. B. Morrill and L. L. Santos (1985).

of a single layer of 1000 to 2000 cells surrounding the blastocoel. During a precursor stage, a region of this shell, the vegetal plate, begins to flatten and thicken while the cohesion of the cells in this region is reduced. There is then formation of a depression when the curvature of the vegetal plate reverses (fig. 5a). The depressed region then extends and invaginates, becoming the archenteron, a tube penetrating into the blastocoel (fig. 5b). Several different biological hypotheses have been put forward to explain this process. It is not for us to discuss the validity of these hypotheses. We can note, however, that in several of the suggested processes, the primary stage of the invagination (the reversal of curvature) is due to a mechanical buckling. Numerical simulations [16] have confirmed this possibility. What our work suggests is that the second stage, the formation of an invaginated tube, could also be due to a continuation of a buckling process. This would only require that the mechanical properties of the shell be inhomogeneous and that the cohesion of the shell be weaker in the region where the buckling occurs. This condition is known to be met in the vegetal plate of embryos.

* * *

We thank C. Allain, A. Boudaoud, P. Aussillous, D. Quéré and A. Huynh for useful discussions.

REFERENCES

[1] Carlson R. L., Sendelbeck R. L. and Hoff N. J., in *An Experimental Study of the Buckling of a Complete Spherical Shell*, NASA Contractor Report no. 550, 1966.
[2] Hutchinson J. W., *J. Appl. Mech.*, **8** (1967) 49.
[3] Gupta N. K., Easwara Prasad G. L. and Gupta S. K., *Thin-Walled Struct.*, **34** (1999) 2141.
[4] Morrill J. B. and Santos L. L., in *The Cellular and Molecular Biology of Invertebrates Development*, edited by Sawyer R. H. and Showman R. M. (University of South Carolina Press) 1985.
[5] Gao C., Donath E., Moya S., Dudnik V. and Möhwald H., *Eur. Phys. J. E*, **5** (2001) 21; Gao C., Leporatti S., Moya S., Donath E. and Möhwald H., *Langmuir*, **17** (2001) 3491.
[6] Pauchard L. and Allain C., *Europhys. Lett.*, **62** (2003) 897; Gorand Y., Pauchard L., Calligari G., Hulin J. P. and Allain C., to be published in *Langmuir*.
[7] Pauchard L. and Allain C., *C. R. Phys.*, **4** (2003) 231.
[8] Cerda E., Ravi-Chandar K. and Mahadevan L., *Nature (London)*, **419** (2002) 579.
[9] Quéré D., *Nature Mater.*, **1** (2002) 14.
[10] Deegan R. D., Bakajin O., Dupont T. F., Huber G., Nager S. R. and Witten T., *Nature*, **389** (1997) 827.
[11] Landau L. and Lifshitz E. M., *Theory of Elasticity*, 3rd edition (Pergamon Press, New York) 1986.
[12] The free diffusion coefficient of colloidal particles for dilute and non-interacting systems is given by $D = k_{\mathrm{B}}T/6\eta_0 a$, where a is the particle diameter and η_0 the solvent viscosity.
[13] This process was observed in the drying of a hydro-soluble polymer solution, Dextran, deposited on super-hydrophobic substrates. In that case, the resulting rigid glassy shell being transparent, the growth of a basal bubble inside the drop is observed directly.
[14] Zarzycki J., *J. Non-Crist. Solids*, **100** (1988) 359.
[15] Pauchard L. and Rica S., *Philos. Mag. B*, **78** (1998) 225.
[16] Davidson L. A., Koehl M. A., Keller R. and Oster G. F., *Development*, **121** (1995) 2005.